# Local sleep in songbirds: Different simultaneous sleep states across the avian pallium

Hamed Yeganegi[1,2], Janie M. Ondracek[1*]

1 Technical University of Munich, TUM School of Life Sciences, Chair of Zoology, Liesel-Beckmann-Str. 4, 85354 Freising-Weihenstephan, Germany.
2 Graduate School of Systemic Neurosciences, Ludwig-Maximilians-University Munich, Großhaderner Str. 2, 82152 Planegg, Germany.
* Correspondence: Janie M. Ondracek, Technical University of Munich, TUM School of Life Sciences, Chair of Zoology, Liesel-Beckmann-Str. 4, 85354 Freising-Weihenstephan, Germany Email: janie.ondracek@tum.de

## Summary

Wakefulness and sleep have often been treated as distinct and global brain states. However, an emerging body of evidence on the local regulation of sleep stages challenges this conventional view. Apart from unihemispheric sleep, the current data that support local variations of neural oscillations during sleep are focused on the homeostatic regulation of local sleep, i.e., the role preceding awake activity. Here, to examine local differences in brain activity during natural sleep, we recorded the electroencephalogram (EEG) and the local field potential (LFP) across multiple sites within the avian pallium of zebra finches without perturbing the previous awake state. We scored the sleep stages independently in each pallial site and found that the overall percentage of slow wave sleep (SWS) was significantly higher, and that SWS durations were significantly longer, in the deeper mesopallium sites compared to most sites on the pallial surface. We analyzed the likelihood of observing simultaneous sleep states across electrodes, and found that on average, sleep stages are not pallium-wide phenomena, but rather deviate widely across electrode sites. Importantly, deeper electrode sites had a dominant role in defining the temporal aspects of sleep state congruence. Altogether, these findings show that local regulation of sleep oscillations also occurs in the avian brain without prior awake recruitment of specific pallial circuits and in the absence of mammalian cortical neural architecture.

## Keywords

Local sleep, sleep stages, avian brain, avian sleep, sleep regulation, cortical regulation of sleep,

## Introduction

During sleep, electroencephalogram (EEG) recordings show that the brain oscillates between two principal states: rapid eye movement sleep (REM) and non-REM (NREM) sleep, which encompasses slow-wave sleep (SWS). Brain activity during REM sleep resembles the awake state: low amplitude and aperiodic electrical activity, which is often accompanied by rapid eye movements in mammals. In contrast, NREM sleep is characterized by the emergence of large amplitude periodic waves and “slow” wave activity during SWS.

REM and NREM sleep stages are conventionally described as distinct states of brain activity that affect the whole brain uniformly and simultaneously. However, recent work on “local sleep” (Huber et al., 2004; Krueger et al., 2019; Vyazovskiy et al., 2011) and unilateral sleep (Mukhametov, 1987; Oleksenko et al., 1992; Rattenborg et al., 1999, 2016) has challenged this notion, suggesting that brain activity during sleep is much more complex.

One well-documented type of non-global sleep is unihemispheric slow wave sleep (USWS), sometimes identified as “asymmetrical sleep” (see (Mascetti, 2016) for a review). This type of sleep has been documented in birds (Ookawa, 2004; Peters et al., 1965; Rattenborg et al., 1999, 2016; Szymczak et al., 1996) and marine mammals (Lyamin et al., 2002; Lyamin, Lapierre, et al., 2008; Lyamin, Manger, et al., 2008; Rattenborg, 2023; Siegel, 2008) and presumably offers the adaptive advantage of sustaining an elevated level of vigilance in response to predation risk (Rattenborg et al., 1999) or the maintenance of swimming or flight control while sleeping (Rattenborg et al., 2016; Siegel, 2008).

Beyond asymmetrical sleep, local variations in neural activity exist during sleep, and they are often distinct from the interhemispheric disparities observed during USWS. Local differences in neural activity have been observed across cortical areas in humans, rodents, and birds (Durán et al., 2018; Emrick et al., 2016; Funk et al., 2016; Nir et al., 2011; Tamaki et al., 2016; V. V. Vyazovskiy et al., 2011) (see (Lesku & Rattenborg, 2014) for a concise overview of avian sleep and (Rattenborg et al., 2019) for a review of local sleep in birds). In particular, slow wave activity (i.e., EEG oscillations below 4 Hz) has been shown to be regulated in a use-dependent, homeostatic manner that is dependent on prior awake activity in both birds and

mammals (Hanlon et al., 2009; Kattler et al., 1994; Rattenborg et al., 2019; V. Vyazovskiy et al., 2000; V. V. Vyazovskiy & Tobler, 2008).

However, sometimes local differences cannot be exclusively attributed to homeostatic mechanisms alone (Durán et al., 2018; Rattenborg et al., 1999). Indeed, local differences in sleep, particularly the local appearance of slow wave activity and sleep spindles (brief bursts of activity at approximately 7-14 Hz), have been observed during natural sleep of humans and rats (Nir et al., 2011; V. V. Vyazovskiy et al., 2011). Moreover, the *intrusion* of slow waves into the globally awake brain has been linked to diminished performance in behavioral tasks in rats and is even termed *local sleep*. Collectively, these observations render the brain-wide delineation between wakefulness and sleep and between NREM and REM sleep unclear. In addition, the exact neural mechanisms orchestrating the transition between wakefulness and NREM sleep, and between NREM and REM sleep in the mammalian brain are still being established (Scammell et al., 2017).

The predominant perspective concerning the neural orchestration of sleep stage transitions has primarily concentrated on the contributions of a limited subset of subcortical regions. These areas encompass a subset of neuronal populations within the brain stem, hypothalamus, and basal forebrain in the case of NREM sleep control, and pontine and hypothalamic subpopulations in the case of REM sleep control (Scammell et al., 2017). This top-down understanding of sleep regulation considers wakefulness and sleep as well-defined, brain-wide states, and models the neural mechanism of sleep control as a switch, akin to an electrical flip-flop switch (Saper et al., 2010). As such, we are faced with an overarching question regarding the central versus local regulation of sleep. That is, how do local instances of pallial sleep contribute to the subpallial central regulation of sleep to induce a global behavioral state in an animal?

To address this query we first need to acquire a comprehensive understanding of the neural oscillations typical of sleep EEG. The theoretical models that deal with the generation of EEG oscillations heavily rely on the mammalian layered structure of cortex (da Silva, 2010). However, the avian pallium, e.g. that of zebra finch, also exhibit sleep EEG oscillations comparable to that of the mammalian brain, despite the absence of a layered cortex (Low et al., 2008; Yeganegi & Ondracek, 2023). Therefore, to better understand the extent of local sleep oscillations across the pallium, it is of great importance to simultaneously probe multiple sites within the avian pallium during sleep. While local regulation of neural activity during sleep in birds has been previously shown to rely on homeostatic regulation (Lesku et al., 2011), it is not known to what extent local differences exist across pallium without perturbing awake activity. To address this question, we examined local differences during natrual sleep using surface EEGs and deep LFP electrodes in four zebra finches.

# Methods

### Experimental animals

All experimental procedures were conducted in adherence to the principles of laboratory animal care and were carried out in compliance with the current versions of the German and European laws on Animal Experimentation (Approval # ROB-55.2-2532.Vet_02-18-108: J.M.O.). Additionally, the experiments followed the guidelines set forth by ARRIVE (Animal Research: Reporting of In Vivo Experiments). Ethical approval for the study was obtained from the ethics committee of the Government of Upper Bavaria (Regierung von Oberbayern), which operates in accordance with § 14.1 TierSchG (German animal welfare law). Furthermore, the housing and breeding arrangements for the animals received the approval of the Veterinary Office of Freising, Germany (Approval # 32-568).

Recordings were acquired from four male zebra finches (*Taeniopygia guttata*) aged 74-91 days post-hatch, all of which exhibited physical signs of maturity as indicated by feather and beak coloring. Details concerning the age and corresponding symbol used for each individual are presented in Table 1.

| Bird ID | Age (dph) | Symbol used in this text | #good electrodes |
|---|---|---|---|
| w025 | 74 | × | 5 |
| w027 | 83 | ○ | 5 |
| w042 | 90 | + | 4 |
| w044 | 91 | ◊ | 5 |

Table. 1 **Description of experimental birds used in experiments.** Bird ID, age in days post-hatch (dph), the corresponding symbol used in the figures, and the number of non-noisy recording electrodes are shown.

Prior to the experiments, the birds were housed in aviaries with a 12:12-hour light:dark cycle. They were provided with access to a seed mix, millet, sepia bone, and water *ad libitum*. Additionally, fresh vegetables and cooked eggs were supplied to the

birds once a week. The recording chambers were equipped with LED lights, UV bird lights (Bird Systems, Germany), infrared LED panels (850 nm waves), and ventilation to ensure continuous air circulation.

**Electrode preparation and positioning**

For each animal, an electrode implant that consisted of 4 EEG electrodes, 4-8 LFP electrodes, a ground and a reference electrode was constructed. The preparation and positioning of the EEG electrodes is described in (Yeganegi & Ondracek, 2023). The LFP electrodes were made from 5 mm lengths of coated steel wire with a bare diameter of 127 µm (A-M Systems, Sequim, WA) and pinned to an omnetics connector with small gold EIB pins (Neuralynx Inc, Bozeman, MT, USA). The signal from the most medial LFP electrode was used from each bird in all analysis.

**Anesthesia and Surgery**

The birds were anesthetized using oxygenated isoflurane gas (EverFlo OPI, Phillips, Netherlands) with a 3-4% concentration during induction and 0.8-1.5% during maintenance. A small tube was used to deliver the anesthetic gas through the bird's beak via a vaporizer (Isotec 4, Groppler, Germany). To prevent the accumulation of excess anesthetic gas, a scavenger (Scavenger LAS, Groppler, Germany) was employed for suctioning. The bird was positioned on a heating pad with a closed-loop temperature monitoring device (Harvard Apparatus, MA, USA). Throughout anesthesia, body temperature was continuously monitored (EVENTEK E300, Shenzhen Shengya Hardware Products Co, China) using an infrared thermometer, ensuring that it remained above 39.5°C.

The anesthetized bird was positioned in a stereotaxic frame (Kopf Instruments, CA, USA) and the head was immobilized. Anesthetic depth assessment was carried out by applying slight pressures on a toe using tweezers. When the toe reflex ceased, we removed the feathers over the head with forceps and made an incision along the sagittal midline. A dental drill (Volvere i7, NSK Europe GmbH, Germany) was used to make small holes in the skull for the EEG electrodes (see the schematic in Fig. 1a) and a small craniotomy (1×1.5 mm) for the LFP electrodes. After the dura matter was removed, the LFP electrodes were lowered 1.8-2.2 mm deep into the pallium, targeting the mesopallium of the dorsal ventricular ridge (DVR) (see the histology sample in Fig. 1b) and secured in place with dental cement (Paladur, Henry Schein Dental, Germany). The EEG electrodes were then positioned and secured with dental cement.

The LFP electrodes were positioned in a row orthogonal to the midline plane, where the LFP electrode closest to the midline was positioned 1.5 mm lateral from the midline, and the LFP electrode most lateral was positioned 2.5 mm lateral from the midline. LFP electrodes were 2-3 mm frontal to the junction between the frontal and parietal cranial bones. The two frontal EEG electrodes were positioned 2 mm lateral from the midline on each side and 5 mm anterior to the junction of frontal and parietal cranial bones. Posterior EEG electrodes were placed at 2.5 mm lateral to the midline and 1 mm posterior to the frontal and parietal bones junction.

After the surgery, animals were released from the stereotaxic frame and administered an analgesic (Metamizole (100-150 mg/kg, i.m.). Animals were kept on the heating pad until signs of recovery from the anesthesia were observed. Following the surgery, an antibiotic (Baytril, 1025 mg/kg, i.m.) and an analgesic (Carprofen, 4 mg/kg, i.m.) were administered for up to 3 days.

**Electrophysiology**

After surgery, the birds were habituated to the implant within the recording chambers. For a recording session, the preamplifier (Intan Technologies, RHD2132) and its associated tether cable were connected to the implanted headstage one hour before the lights were turned off (light-off period: 10:00 PM - 10:00 AM) to allow the birds to adopt a natural sleep posture. The tether weight was counterbalanced using an elastic rubber band. Electrode signals were acquired with a sampling rate of 30 kHz using an Open Ephys data acquisition board (OEPS, Portugal), filtered within the range of 0.1-9987 Hz, and saved in the Open Ephys GUI ".continuous" format. A near-infrared sensitive camera (acA1300-60gm, Basler Ag, Germany) was used to acquire video recordings of the animals using custom-written software (ZR View, Robert Zollner). Frames were triggered using a pulse generator (Pulse Pal, Sanworks, NY, USA (35)) at a frame rate of 20 Hz. The tether cable was disconnected from the headstage half an hour after the lights were turned on the following morning.

**Histology**

After the final recording session, the birds were deeply anesthetized using a lethal dose of sodium pentobarbital (250 mg/kg, i.m.). Once the corneal reflex and heartbeat had ceased, the bird was decapitated and the brain was extracted from the skull. Subsequently, the brain was immersed in a 4% formaldehyde solution in phosphate-buffered saline for a minimum duration of one day. 80 µm coronal sections were stained with cresyl violet to aid in electrode site verification.

### Data Analysis

Birds were recorded for a period of at least two weeks. The recordings analyzed in this study all ocurred after at least one week of habituation. For data analysis, one whole night of sleep was used for each bird. The night of data was selected based on the behavior (sleep was consolidated), the quality of electrophysiology data, and the quality of the video recording (the bird was within the recording frame throughout the night).

### Automatic sleep staging

All data analysis was conducted offline in Matlab (Matworks, Inc., Natick, MA). Electrophysiological data were down-sampled to 468.75 samples/sec (equivalent to a down-sampling factor of 64). Similar to previous work (Yeganegi & Ondracek, 2023), an automatic sleep staging procedure was employed to classify each 3-second data window into one of the following categories: wake, SWS, REM, or Intermediate Sleep (IS). IS can be considered a transitional stage of NREM sleep, and it typically lacks the large slow oscillations that characterize SWS (Low et al., 2008). In a first pass, the distinction between wake and sleep was determined by examining each 3-s bin for a significant movement artifact (EEG amplitude >4 inter-quartile above the baseline). Movement was confirmed by inspecting the corresponding video recordings; movement artifacts typically involved body twitches, eye opening, or changes in posture. After this first pass (wake versus sleep), the algorithm described in (Low et al., 2008) and (Canavan & Margoliash, 2020) was used to assign sleep stages to the sleep bins.

### Sleep stage congruence

To quantify differences in neural activity across different brain regions, we first scored the sleep separately in each of the five electrode sites: right and left EEG, right and left caudal EEG, and the medial-most LFP electrode in DVR. Then, we used the definition of congruence as stated in (Durán et al., 2018); that is, “congruence” was defined as the percentage with which a given channel shows the same sleep stage as a baseline comparison channel. We chose the left frontal EEG electrode as the baseline electrode, similar to (Durán et al., 2018). Congruence was then computed for each electrode comparison and each stage of sleep. For example, to determine the congruence between the right caudal electrode and the baseline electrode during SWS, we identified all of the 3-s bins that were labeled as SWS in the baseline electrode, and then calculated the percentage of those bins that were also labeled as SWS in the right caudal electrode. If all SWS bins in the baseline electrode corresponded to matching SWS binds in the comparison electrode, then the congruence was 100%. If some of those bins do not match, i.e., a SWS bin in the baseline electrode is labeled as a IS bin in the comparison electrode, then the congruence will be less than 100%. We also computed the congruence in sliding windows. The window length was set to five minutes, so that we had enough bins of each stage of sleep for the congruence calculation while maintaining a high temporal resolution.

### Spectral analysis

Power spectral analysis was computed using the Welch method on each 3-sec window of SWS in different channels. The number of discrete Fourier transform (DFT) points to use in the PSD estimate was set to 512. The 95% confidence interval was then estimated via computation of standard error as described in (Altman & Bland, 2005). To compute the spectrograms visualized in Fig. 1D, the continuous wavelet transform (cwt function in Matlab) was used with the Gabor kernel.

### Statistical analysis

The difference between the time spent in each stage of sleep at different recording sites was assessed using analyses of variance (ANOVA) test with the recording site as factor. The ANOVA tests were followed by post hoc Tukey multiple comparison, to evaluate the significance of differences between any pair of the recording sites. An identical process was followed to compare the differences in the duration of the episodes of each stage between sites. A p-value of <0.05 was considered significant. To ANOVA output tables for all tests are reported in the supplementary file.

## Results

We recorded the surface EEG, as well as the deep LFP within the pallial domain, in four zebra finches. Two silver ball electrodes recorded surface EEG activity in anterior and posterior sites in each hemisphere (four EEG electrodes in total) (Fig. 1A). In addition, 4-8 steel electrodes recorded the LFP in the DVR (Fig. 1A and 1B). During sleep, both surface and LFP electrodes showed brain oscillations typical of sleep, i.e., alternative periods of high amplitude slow wave activity, periods of low amplitude gamma oscillations, and periods of mixed frequency EEG activity. A 15-sec trace of EEG and LFP activity during sleep is depicted in Fig. 1C.

As a whole, the EEG and LFP activity was highly heterogeneous across sites: high-amplitude peaks, deflections, and bursts of activity appeared on only one EEG electrode or only in the LFP recordings. More interestingly, however, was the observation of sustained periods of time when different oscillations appeared simultaneously across different sites. To better characterize

these local differences in neural activity, we segmented the EEG or LFP into discrete stages for each electrode separately (supplementary Fig. S1 and Fig. 1D). We labeled each 3-sec bin of neural activity as either of wake, SWS, IS, or REM sleep (Fig. 1D). The differences in sleep stages, as scored individually across different sites, correspond with the local variations in the spectral composition of the neural activity at these sites (see spectrograms in Fig. 1D).

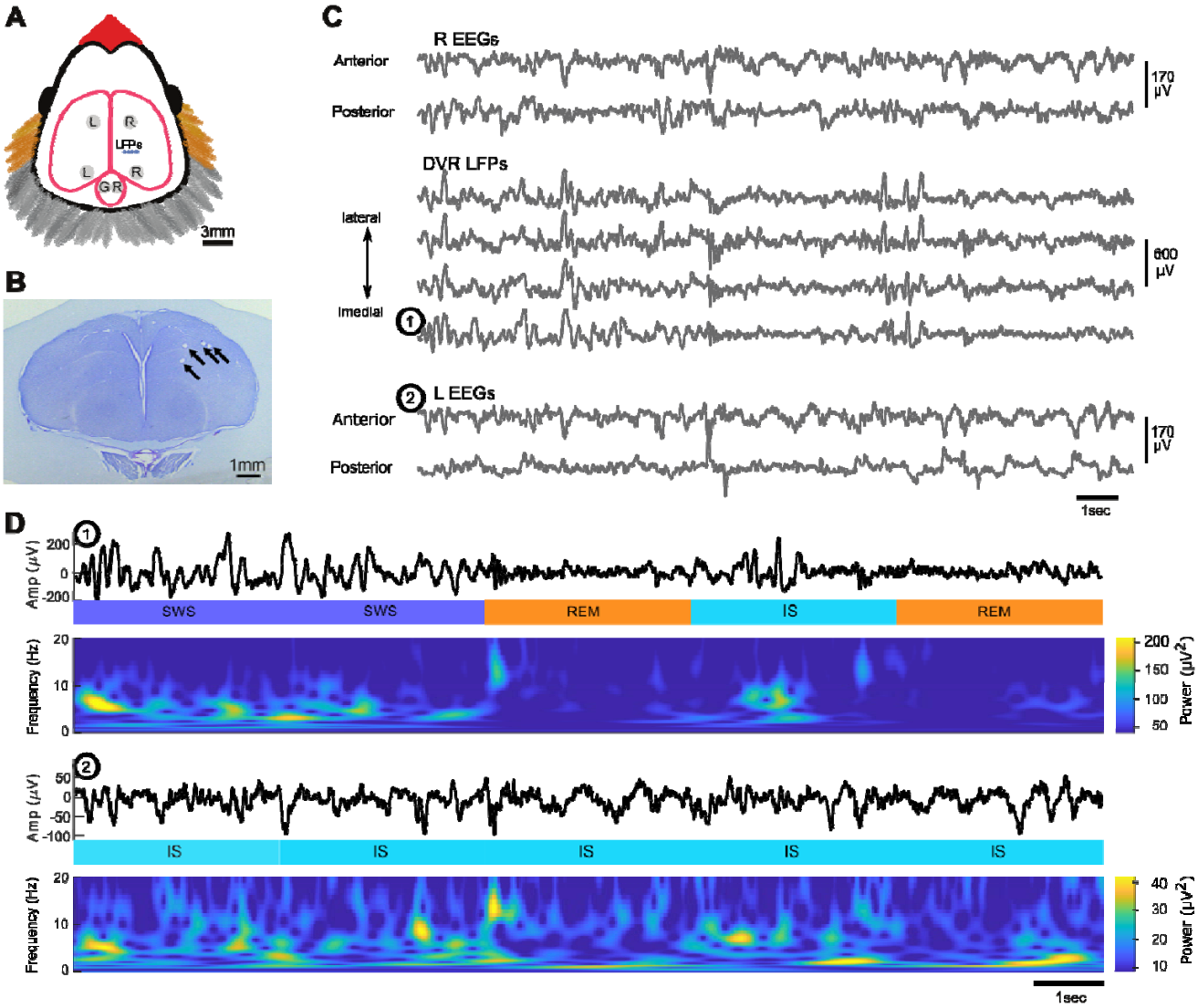


**Fig. 1 Local variations in sleep oscillations across pallial areas.** (A) The schematic depicts the locations of the EEG and LFP electrodes (n=4 birds). Electrodes consist of four surface EEG electrodes, two on each hemisphere on the right and left, and 4-8 deep LFP electrodes in the right hemisphere. For the data analysis, only the most medial LFP electrode was used. (B) Histological section (bird w042) depicts LFP electrode tracts (black arrows). Electrode tips were 1.8-2.2 mm deep in the mesopallium of the DVR. (C) Simultaneous recordings across different sites and depths reveal local variations in sleep oscillations across pallial areas, with notable differences between surface and depth electrodes. LFP traces from top to bottom correspond to sites from most lateral to most medial. (D) Simultaneously recorded LFP trace (1) and left anterior EEG trace (2) with corresponding sleep stage labels (colored bars) and spectrograms (bottom panels). The differences in the spectrograms highlight the variable spectral content across electrode sites and contribute to the different sleep stage labels. IS: Intermediate Stage. DVR: Dorsal Ventricular Ridge.

First, we compared the overall percentage of time spent in each sleep stage for all recording sites. We observed a significant difference across electrode sites for the overall percentage of time spent in SWS ($F(4, 14) = 5.68$, $p = 0.0063$). A post-hoc Tukey multiple comparison test revealed that the percentage of time spent in SWS differed between the DVR and three

superficial sites, namely, the left anterior EEG ($p = 0.012$), right anterior EEG ($p = 0.010$), and right posterior EEG ($p = 0.012$). We did not observe significant differences across the electrodes sites for IS or REM stages ($F(4, 14) = 1.88$, $p = 0.17$ and $F(4, 14) = 1.16$, $p = 0.37$, respectively; one-way ANOVA).

We also compared the duration of time spent in SWS, IS, and REM sleep across the different recording sites. For all stages of sleep, we observed significant differences across electrode sites (Fig. 2B; refer to the supplementary material for statistical tests). In particular, the durations of time spent in SWS and IS were significantly different across electrode sites..

Altogether, we observed an overall higher percentage of time and longer durations of SWS recorded in the DVR compared to the superficial sites, suggesting that slow waves may originate from deeper sites within the DVR (or elsewhere) and spread to the pallial surface (see Discussion for more details).

Given the observation of significant differences in the proportion of SWS in the DVR compared to the superficial pallial sites (Fig. 2A), the question arises as to whether the SWS has identical spectral features across all channels or differs in the spectral content. To test this hypothesis, we compared the relative spectral density (relative PSD) of SWS episodes across sites (Supplementary Fig. S2). We observed that the spectral content of EEG during the SWS stage differed between electrode sites and was characterized by high inter-subject variability in the spectral content of the SWS.

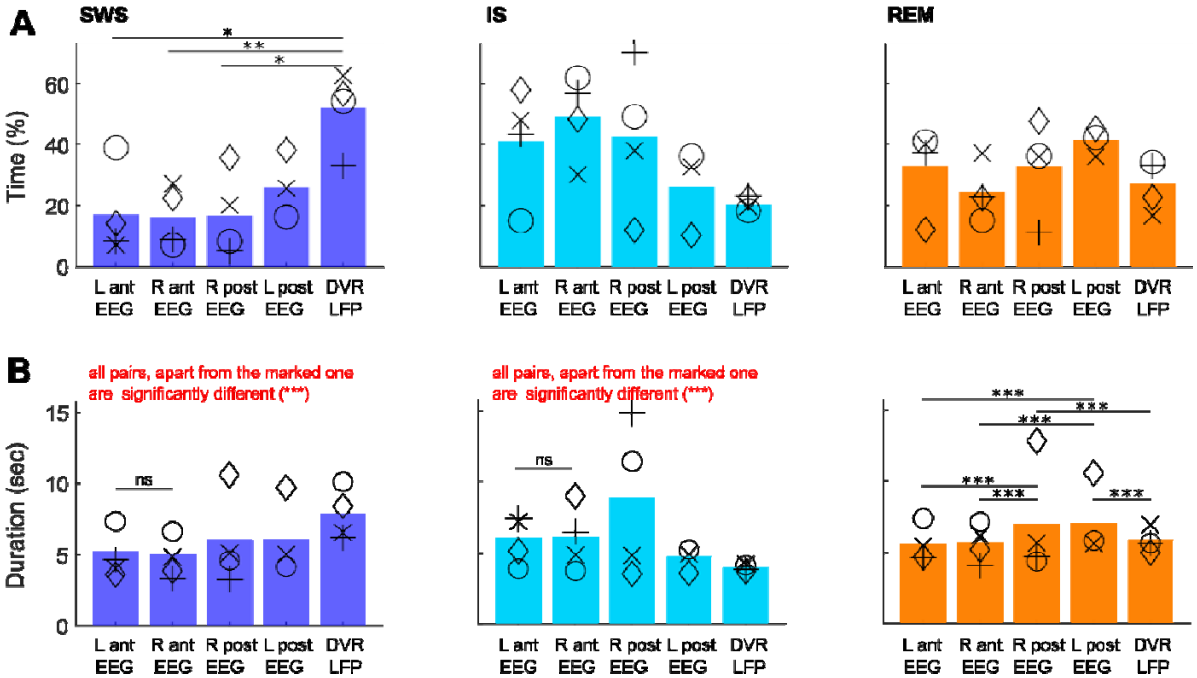


**Fig. 2 Sleep stage durations vary as a function of location.** (A) Sleep stage percentages across recording sites. Although the percentage of time spent in IS and REM sleep was not significantly different across sites (see text for details), the percentage of time spent in SWS was significantly different across sites. Bars denote mean across birds; markers correspond to individual birds (see Table 1 for details). (B) Duration of SWS, IS, and REM sleep across recording sites. Notably, sleep stage durations were significantly different as a function of location, particularly for SWS and IS stages.

We were curious as to how frequently different electrode sites shared the same sleep stage at the same time. Similar to (12), we quantified the congruence (Fig. 3) between each electrode and a designated baseline electrode. Here, similar to (12) we chose the left frontal EEG electrode as the baseline electrode (Fig. 3A). The congruence is an estimate of the likelihood that two electrodes share the sleep state (see Methods for details). Congruence values less than 100% indicate a difference between the two electrodes and thus identify local differences in sleep stages. The congruence values for each electrode and for each sleep stage are presented in Fig. 3B. We observed that for all sleep stages and across all electrodes, the congruence did not surpass 59.0%. This implies that the neural oscillations observed during sleep are, to a large extent, local and occur within a small anatomical network. In other words, a given sleep stage is not necessarily a brain-wide phenomenon.

Next, we hypothesized that the congruence is not a stationary value, but changes over sleep time. To explore the temporal dynamics of congruence, we computed congruence in 5-minute sliding windows. We focused on the congruence between the

DVR and the baseline electrode since the DVR electrode showed the maximum congruence during SWS and the minimum congruence during IS among all electrodes (see Fig. 3B) and was the only site with a significantly higher proportion of SWS compared to all other sites (see Fig. 2A). We observed that the temporal congruence between the DVR and the baseline electrode did indeed change throughout the sleep time and was dependent on the stage of sleep in the baseline and the DVR electrodes (Fig. 3C and Fig. 3D).

During the night, the congruence between the DVR and baseline electrode decreased for SWS and increased for REM sleep (Fig. 3E and Fig. 3F). This temporal dynamic was closely coupled to the temporal dynamics SWS and REM sleep in DVR, and not in the baseline channel. To test this, we calculated the correlation coefficient between the sleep-state congruence and the probability of the sleep stage for both SWS and REM sleep. For the DVR electrode, the correlation coefficient was high for congruence and SWS and REM sleep comparisons when calculated using the DVR p(SWS) and p(REM): 0.86 ± 0.12 for SWS (mean and sd among birds) and 0.93 ± 0.04 for REM sleep. In contrast, the correlation coefficient was low for congruence and SWS and REM sleep comparisons when calculated using the baseline electrode p(SWS) and p(REM): 0.47 ± 0.18 for SWS (mean and sd among birds) and 0.52 ± 0.31 for REM.

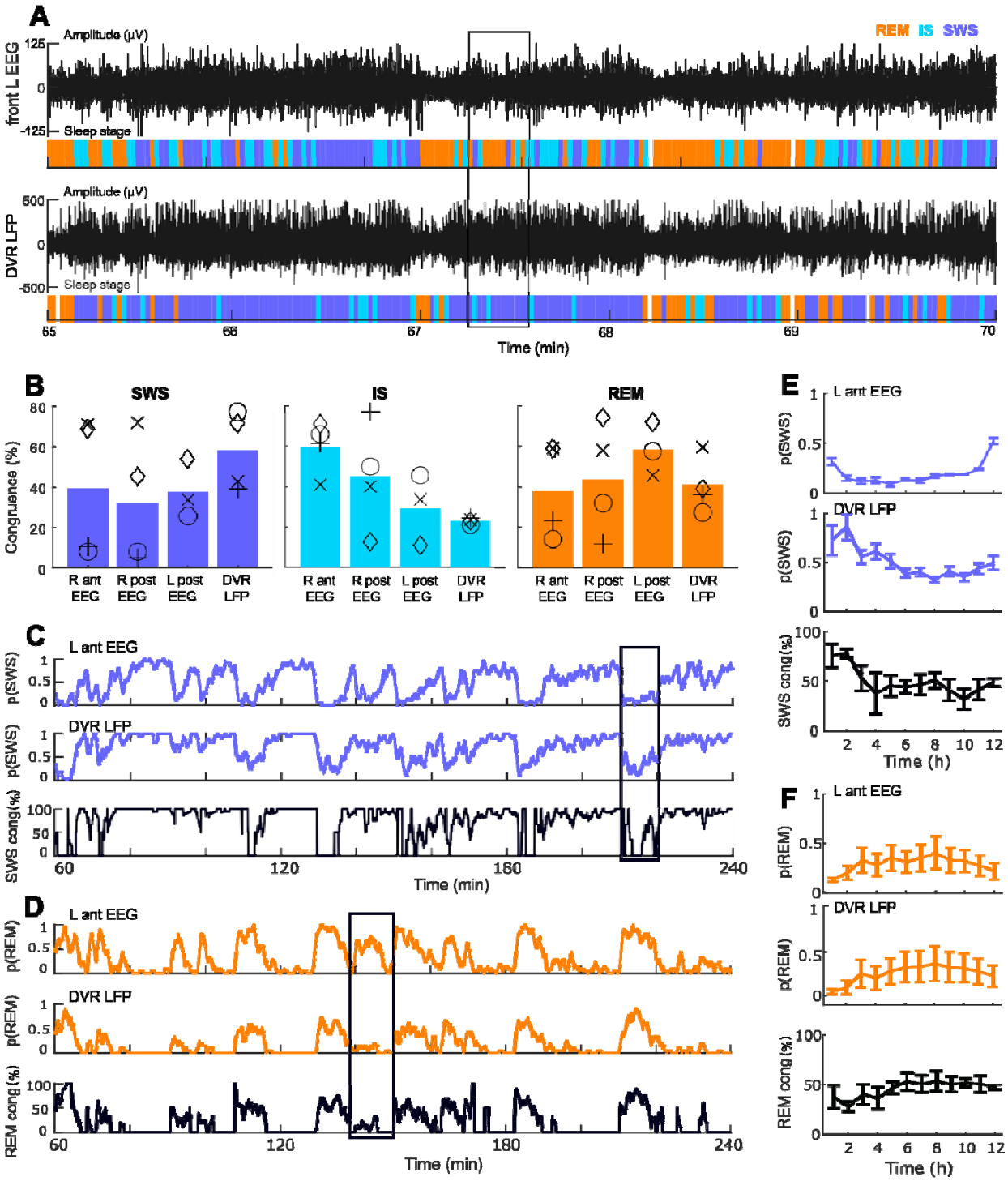


**Fig. 3 Quantification of local differences in sleep stages across the recording sites using congruence.** (A) Sample of simultaneous EEG and LFP recordings (left frontal EEG and LFP in the DVR) displaying differences in identified sleep stages across different sites. Sleep stages were independently scored in 3-second windows at each site, with corresponding sleep stages depicted beneath each signal. Distinct sleep stage differences between sites are visually evident through the color-coded representations of sleep stages for the same time windows. Note, for instance, the marked contrast in sleep stages during the time period enclosed by the rectangular box. (B) Congruence across sites for three sleep stages. Bars denote mean across birds; markers correspond to individual birds (see Table 1). In all cases, the congruence was below 59.0%, suggesting that the sleep stages was location-dependent and not always a brain-wide phenomenon. The lowest congruence was observed in the DVR during IS (23.2%). (C) Temporal dynamics of congruence between DVR and the base electrode during SWS. The probability of the SWS stage in the baseline electrode (upper subplot), the probability of SWS in the DVR (middle subplot), and the

congruence calculated between the electrodes (lower subplot) were computed in 5-minute sliding windows. Congruence changes were closely tied to the probability of SWS in both channels, especially the DVR channel. The rectangle indicates periods of low congruence due to differences between the probability of SWS in the baseline and DVR electrodes. (D) Similar to (C), but for the dynamics of the REM sleep. Note the different time span in the data presented in (C) and (D) with the data in (A). Throughout the night, the congruence in the DVR generally decreases during SWS (E) and increases during REM sleep (F). Correlation coefficients between sleep stage likelihood and congruence were highest for DVR compared to the baseline electrode (see the text), indicating a dominant role for the DVR electrode in defining congruence compared to the baseline channel.

## Discussion

Our findings highlight the presence of local neural oscillations linked to discrete sleep stages across diverse sites within the avian pallium, which is in line with emerging evidence that suggests that sleep may be locally regulated across the brain (Krueger et al., 2008). Local regulation of sleep under homeostatic control has already been demonstrated in birds. In (J. A. Lesku et al., 2011), one eye in the pigeons was covered, while the other eye was presented with a visual stimulus. On the following night, after the asymmetric visual exposure, EEG was recorded during sleep from the left and right hemispheres. The slow wave activity increased only in the hemisphere contralateral to the visually stimulated eye, demonstrating the local regulation of sleep as a homeostatic mechanism. In contrast to these results, our findings show that local differences in sleep also exist after unperturbed awake activity and is not necessarily the result of homeostatic control.

The idea that sleep could be regulated locally challenges conventional theories that favor the concept of brain-wide sleep that is driven by sleep regulatory *centers* (Saper et al., 2010; Scammell et al., 2017). Indeed, recent studies have suggested that sleep may be a default characteristic of neuronal networks, as demonstrated by the observation of sleep-like oscillations in isolated neural tissues (Bandarabadi et al., 2020; Hinard et al., 2012) and relies on preceding (asymmetrical) activity during wakefulness (Huber et al., 2004; Kattler et al., 1994; V. Vyazovskiy et al., 2000). Other studies have suggested that metabolically driven changes in sleep-regulatory substances could also regulate local sleep patterns (Hinard et al., 2012). Finally, mathematical modeling has highlighted that the synchronization of sleep-like states across individual cortical columns could ultimately culminate in brain-wide sleep as an emergent property of local-network interactions, without a need for a central switch (Roy et al., 2008). These recent findings collectively propose that the regulation of sleep might not exclusively hinge on a designated neural circuit that switches whole cortical areas between discrete states. Our observation of distinct sleep stages existing simultaneously across sites within the avian pallium adds evidence to this growing body of emerging data.

The original work that quantified the homogeneity of sleep stages across the cortical sites using congruence was conducted in rats (Durán et al., 2018). In that study, the activity in cortical sites (medial prefrontal, and superficial parietal) and a hippocampal site was compared to a baseline cortical site (superficial frontal). The authors reported average congruence during SWS and REM above 87%. But during IS sleep, the value dropped to 36%. In comparison, in the zebra finch pallium, we observed that the average congruence over all three stages was not higher than 59%, without a significant distinction between the IS and the SWS and REM stages (see Fig. 2A). As such, we have found a much higher level of heterogeneity in the sleep stages across avian pallium as compared to the mammalian brain.

This observation could be explained considering the differences in the pallial designs between the mammalian and avian brains, most prominently the laminar organization of cortical areas and the presence of the corpus callosum in the placental mammal's brain. However, there are caveats to this explanation. First, the technical differences in sleep scoring methods could account for differences in the estimated congruence. Second, in rats, the IS sleep occupied only 2.2% percentage of the time, including the wake period. Here (Fig. 2B), we observed that the IS sleep occupies at least 20% of sleep, not including the wake period, in all channels. Including the light-on period, it still accounts for at least 10% of the time, which is much higher than that of rats. Thirdly, the differences in the recording sites might account for marked differences. For instance, it has been reported that under isoflurane anesthesia, slow waves are present in the nidopallium (a subdivision of avian pallium ventral to mesopallium) but not the avian hippocampus (van der Meij et al., 2020).

Finally, our data has implications regarding the origin of slow waves in the avian pallium. We observed that both the percentage and duration of SWS are higher for the electrodes in the mesopallium compared to the electrodes on the pallial surface. In the context of the mammalian brain, slow oscillations seem to emerge from various neocortical regions, subsequently propagating horizontally across the neocortex akin to a traveling wave (Murphy et al., 2009; Nir et al., 2011). Although the neocortex possesses the inherent capacity to generate slow oscillations after recovery from thalamotomy, thalamic input plays a critical role in the generation of slow waves under normal physiological circumstances (Crunelli & Hughes, 2010; Lemieux et al., 2014). Notably, the inception of slow waves tends to manifest predominantly within layer 5, a

layer that receives inputs from the thalamus (Constantinople & Bruno, 2013), and subsequently propagates vertically within cortical columns (Capone et al., 2019).

In the avian brain, two subregions of the visual hyperpallium are known to receive extensive thalamic input, namely the Interstitial part of the apical hyperpallium and the intercalated part of the hyperpallium (Reiner et al., 2004; Wild, 1987). A multichannel LFP recording that allowed simultaneous recordings from these two regions as well as a subregion with far less thalamic input, i.e., hyperpallium densocellulare, showed that the amplitude of slow waves was higher in the thalamic recipient subdivisions (Van Der Meij et al., 2019). In addition, it was reported that the slow waves tend to appear first in these subdivisions and then propagate through, and outward, from these areas. Slow wave amplitude during sleep has not been directly investigated in the songbird pallium, which also receives extensive thalamic input to brain areas involved in vocal learning (Akutagawa & Konishi, 2005; Boettiger & Doupe, 1998; Coleman et al., 2007; Ondracek & Hahnloser, 2013).

Could local EEG patterns be regulated by thalamic input, or is it instead locally regulated by the pallium itself? Given the distinctions between the mammalian cortex and the avian pallium, further investigations are necessary to elucidate the underlying mechanisms responsible for the genesis of slow waves and their local modulations in the avian brain.

## Author Contributions

Conceptualization, H.Y. and J.M.O.; Methodology, H.Y. and J.M.O.; Software: H.Y. and J.M.O.; Validation, J.M.O.; Formal Analysis, H.Y.; Investigation, H.Y.; Writing – Original Draft, H.Y.; Writing – Review & Editing, J.M.O.; Funding Acquisition, J.M.O.; Resources, J.M.O.; Visualization, H.Y. and J.M.O.; Supervision, J.M.O.; Project Administration, J.M.O.

## Acknowledgements

The authors are thankful to B. Seibel and Y. Schwarz for technical assistance; C. Fink and E. Jochen for help with mechanical design, fabrication, and electronics; A. Schuhbauer for administrative assistance, and H. Luksch, for feedback and support of this research.

## Funding Information

This study was funded by grants from the German Research Foundation (Deutsche Forschungsgemeinschaft; ON 151/1-1) and the Daimler and Benz Foundation (Postdoctoral scholarship) awarded to Janie M. Ondracek.

## Conflict of Interest Statement

The authors declare no conflicts of interest related to this work.

## Data Availability Statement

The data that support the findings will be available in upon request from the corresponding author.

## ORCID

Hamed Yeganegi https://orcid.org/0000-0002-1737-0038

Janie M. Ondracek https://orcid.org/0000-0002-4570-447X

## References

Akutagawa, E., & Konishi, M. (2005). Connections of thalamic modulatory centers to the vocal control system of the zebra finch. *Proceedings of the National Academy of Sciences of the United States of America*, *102*(39), 14086–14091. https://doi.org/10.1073/pnas.0506774102

Altman, D. G., & Bland, J. M. (2005). Standard deviations and standard errors. *BMJ (Clinical Research Ed.)*, *331*(7521), 903. https://doi.org/10.1136/bmj.331.7521.903

Bandarabadi, M., Vassalli, A., & Tafti, M. (2020). Sleep as a default state of cortical and subcortical networks. *Current Opinion in Physiology*, *15*, 60–67. https://doi.org/10.1016/j.cophys.2019.12.004

Boettiger, C. A., & Doupe, A. J. (1998). Intrinsic and Thalamic Excitatory Inputs Onto Songbird LMAN Neurons Differ in Their Pharmacological and Temporal Properties. *Journal of Neurophysiology*, *79*(5), 2615–2628. https://doi.org/10.1152/jn.1998.79.5.2615

Canavan, S. V., & Margoliash, D. (2020). Budgerigars have complex sleep structure similar to that of mammals. *PLOS Biology*, *18*(11), e3000929. https://doi.org/10.1371/journal.pbio.3000929

Capone, C., Rebollo, B., Muñoz, A., Illa, X., Del Giudice, P., Sanchez-Vives, M. V., & Mattia, M. (2019). Slow Waves in Cortical Slices: How Spontaneous Activity is Shaped by Laminar Structure. *Cerebral Cortex (New York, N.Y.: 1991)*, *29*(1), 319–335. https://doi.org/10.1093/cercor/bhx326

Coleman, M. J., Roy, A., Wild, J. M., & Mooney, R. (2007). Thalamic gating of auditory responses in telencephalic song control nuclei. *The Journal of Neuroscience: The Official Journal of the Society for Neuroscience*, *27*(37), 10024–10036. https://doi.org/10.1523/JNEUROSCI.2215-07.2007

Constantinople, C. M., & Bruno, R. M. (2013). Deep cortical layers are activated directly by thalamus. *Science (New York, N.Y.)*, *340*(6140), 1591–1594. https://doi.org/10.1126/science.1236425

Crunelli, V., & Hughes, S. W. (2010). The slow (<1 Hz) rhythm of non-REM sleep: A dialogue between three cardinal oscillators. *Nature Neuroscience*, *13*(1), 9–17. https://doi.org/10.1038/nn.2445

da Silva, F. L. (2010). EEG: Origin and Measurement. In C. Mulert & L. Lemieux (Eds.), *EEG - fMRI: Physiological Basis, Technique, and Applications* (pp. 19–38). Springer. https://doi.org/10.1007/978-3-540-87919-0_2

Durán, E., Oyanedel, C. N., Niethard, N., Inostroza, M., & Born, J. (2018). Sleep stage dynamics in neocortex and hippocampus. *Sleep*, *41*(6). https://doi.org/10.1093/sleep/zsy060

Emrick, J. J., Gross, B. A., Riley, B. T., & Poe, G. R. (2016). Different Simultaneous Sleep States in the Hippocampus and Neocortex. *Sleep*, *39*(12), 2201–2209. https://doi.org/10.5665/sleep.6326

Funk, C. M., Honjoh, S., Rodriguez, A. V., Cirelli, C., & Tononi, G. (2016). Local Slow Waves in Superficial Layers of Primary Cortical Areas during REM Sleep. *Current Biology: CB*, *26*(3), 396–403. https://doi.org/10.1016/j.cub.2015.11.062

Hanlon, E. C., Faraguna, U., Vyazovskiy, V. V., Tononi, G., & Cirelli, C. (2009). Effects of skilled training on sleep slow wave activity and cortical gene expression in the rat. *Sleep*, *32*(6), 719–729. https://doi.org/10.1093/sleep/32.6.719

Hinard, V., Mikhail, C., Pradervand, S., Curie, T., Houtkooper, R. H., Auwerx, J., Franken, P., & Tafti, M. (2012). Key electrophysiological, molecular, and metabolic signatures of sleep and wakefulness revealed in primary cortical cultures. *The Journal of Neuroscience: The Official Journal of the Society for Neuroscience*, *32*(36), 12506–12517. https://doi.org/10.1523/JNEUROSCI.2306-12.2012

Huber, R., Ghilardi, M. F., Massimini, M., & Tononi, G. (2004). Local sleep and learning. *Nature*, *430*(6995), 78–81. https://doi.org/10.1038/nature02663

Kattler, H., Dijk, D. J., & Borbély, A. A. (1994). Effect of unilateral somatosensory stimulation prior to sleep on the sleep EEG in humans. *Journal of Sleep Research*, *3*(3), 159–164. https://doi.org/10.1111/j.1365-2869.1994.tb00123.x

Krueger, J. M., Nguyen, J. T., Dykstra-Aiello, C. J., & Taishi, P. (2019). Local sleep. *Sleep Medicine Reviews*, *43*, 14–21. https://doi.org/10.1016/j.smrv.2018.10.001

Krueger, J. M., Rector, D. M., Roy, S., Van Dongen, H. P. A., Belenky, G., & Panksepp, J. (2008). Sleep as a fundamental property of neuronal assemblies. *Nature Reviews Neuroscience*, *9*(12), Article 12. https://doi.org/10.1038/nrn2521

Lemieux, M., Chen, J.-Y., Lonjers, P., Bazhenov, M., & Timofeev, I. (2014). The impact of cortical deafferentation on the neocortical slow oscillation. *The Journal of Neuroscience: The Official Journal of the Society for Neuroscience*, *34*(16), 5689–5703. https://doi.org/10.1523/JNEUROSCI.1156-13.2014

Lesku, J. a., & Rattenborg, N. C. (2014). Avian sleep. *Current Biology*, *24*(1), R12–R14. https://doi.org/10.1016/j.cub.2013.10.005

Lesku, J. A., Vyssotski, A. L., Martinez-Gonzalez, D., Wilzeck, C., & Rattenborg, N. C. (2011). Local sleep homeostasis in the avian brain: Convergence of sleep function in mammals and birds? *Proceedings. Biological Sciences / The Royal Society*, *278*(1717), 2419–2428. https://doi.org/10.1098/rspb.2010.2316

Low, P., Shank, S. S., Sejnowski, T. J., & Margoliash, D. (2008). Mammalian-like features of sleep structure in zebra finches. *Proc Natl Acad Sci U S A*, *105*(26), 9081–9086. https://doi.org/0703452105 [pii]10.1073/pnas.0703452105

Lyamin, O. I., Lapierre, J. L., Kosenko, P. O., Mukhametov, L. M., & Siegel, J. M. (2008). Electroencephalogram asymmetry and spectral power during sleep in the northern fur seal. *Journal of Sleep Research*, *17*(2), 154–165. https://doi.org/10.1111/j.1365-2869.2008.00639.x

Lyamin, O. I., Manger, P. R., Ridgway, S. H., Mukhametov, L. M., & Siegel, J. M. (2008). Cetacean sleep: An unusual form of mammalian sleep. *Neuroscience and Biobehavioral Reviews*, *32*(8), 1451–1484. https://doi.org/10.1016/j.neubiorev.2008.05.023

Lyamin, O. I., Mukhametov, L. M., Siegel, J. M., Nazarenko, E. A., Polyakova, I. G., & Shpak, O. V. (2002). Unihemispheric slow wave sleep and the state of the eyes in a white whale. *Behavioural Brain Research*, *129*(1–2), 125–129. https://doi.org/10.1016/S0166-4328(01)00346-1

Mascetti, G. G. (2016). Unihemispheric sleep and asymmetrical sleep: Behavioral, neurophysiological, and functional perspectives. *Nature and Science of Sleep*, *8*, 221–238. https://doi.org/10.2147/NSS.S71970

Mukhametov, L. M. (1987). Unihemispheric slow-wave sleep in the Amazonian dolphin, Inia geoffrensis. *Neuroscience Letters*, *79*(1), 128–132. https://doi.org/10.1016/0304-3940(87)90684-7

Murphy, M., Riedner, B. A., Huber, R., Massimini, M., Ferrarelli, F., & Tononi, G. (2009). Source modeling sleep slow waves. *Proceedings of the National Academy of Sciences of the United States of America*, *106*(5), 1608–1613. https://doi.org/10.1073/pnas.0807933106

Nir, Y., Staba, R. J., Andrillon, T., Vyazovskiy, V. V., Cirelli, C., Fried, I., & Tononi, G. (2011). Regional Slow Waves and Spindles in Human Sleep. *Neuron*, *70*(1), 153–169. https://doi.org/10.1016/j.neuron.2011.02.043

Oleksenko, A. I., Mukhametov, L. M., Polyakova, I. G., Supin, A. Y., & Kovalzon, V. M. (1992). Unihemispheric sleep deprivation in bottlenose dolphins. *Journal of Sleep Research*, *1*(1), 40–44. https://doi.org/10.1111/j.1365-2869.1992.tb00007.x

Ondracek, J. M., & Hahnloser, R. H. R. (2013). Advances in Understanding the Auditory Brain of Songbirds. In C. Köppl, G. A. Manley, A. N. Popper, & R. R. Fay (Eds.), *Insights from Comparative Hearing Research* (pp. 347–388). Springer New York. https://doi.org/10.1007/2506_2013_31

Ookawa, T. (2004). The electroencephalogram and sleep in the domestic chicken. *Avian and Poultry Biology Reviews*, *15*, 1–8. https://doi.org/10.3184/147020604783637453

Peters, J., Vonderahe, A., & Schmid, D. (1965). Onset of cerebral electrical activity associated with behavioral sleep and attention in the developing chick. *The Journal of Experimental Zoology*, *160*(3), 255–261. https://doi.org/10.1002/jez.1401600303

Rattenborg, N. C. (2023). Diverse sleep strategies at sea. *Science*, *381*(6657), 486–487. https://doi.org/10.1126/science.adh9193

Rattenborg, N. C., Lima, S. L., & Amlaner, C. J. (1999). Facultative control of avian unihemispheric sleep under the risk of predation. *Behavioural Brain Research*, *105*(2), 163–172. https://doi.org/10.1016/S0166-4328(99)00070-4

Rattenborg, N. C., Van Der Meij, J., Beckers, G. J. L., & Lesku, J. A. (2019). Local aspects of avian non-rem and rem sleep. *Frontiers in Neuroscience*, *13*(JUN), 1–16. https://doi.org/10.3389/fnins.2019.00567

Rattenborg, N. C., Voirin, B., Cruz, S. M., Tisdale, R. K., Dell'Omo, G., Lipp, H.-P., Wikelski, M., & Vyssotski, A. L. (2016). Evidence that birds sleep in mid-flight. *Nature Communications*, *7*, 12468. https://doi.org/10.1038/ncomms12468

Reiner, A. J., Perkel, D. J., Bruce, L. L., Butler, A. B., Csillag, A., Kuenzel, W., Medina, L., Paxinos, G., Shimizu, T., Striedter, G. F., Wild, J. M., Ball, G. F., Durand, S. E., Güntürkün, O., Lee, D. W., Mello, C. V., Powers, A. S., White, S. A., Hough, G. E., … Gütürkün, O. (2004). Revised nomenclature for avian telencephalon and some related brainstem nuclei. *The Journal of Comparative Neurology*, *473*(3), 377–414. https://doi.org/10.1002/cne.20118

Roy, S., Krueger, J. M., Rector, D. M., & Wan, Y. (2008). A Network Model for Activity-Dependent Sleep Regulation. *Journal of Theoretical Biology*, *253*(3), 462–468. https://doi.org/10.1016/j.jtbi.2008.03.033

Saper, C. B., Fuller, P. M., Pedersen, N. P., Lu, J., & Scammell, T. E. (2010). Sleep State Switching. *Neuron*, *68*(6), 1023–1042. https://doi.org/10.1016/j.neuron.2010.11.032

Scammell, T. E., Arrigoni, E., & Lipton, J. (2017). Neural Circuitry of Wakefulness and Sleep. *Neuron*, *93*(4), 747–765. https://doi.org/10.1016/j.neuron.2017.01.014

Siegel, J. M. (2008). Do all animals sleep? *Trends in Neurosciences*, *31*(4), 208–213. https://doi.org/10.1016/j.tins.2008.02.001

Szymczak, J. T., Kaiser, W., Helb, H. W., & Beszczyńska, B. (1996). A study of sleep in the European blackbird. *Physiology & Behavior*, *60*(4), 1115–1120. https://doi.org/10.1016/0031-9384(96)00231-4

Tamaki, M., Bang, J. W., Watanabe, T., & Sasaki, Y. (2016). Night Watch in One Brain Hemisphere during Sleep Associated with the First-Night Effect in Humans. *Current Biology: CB*, *26*(9), 1190–1194. https://doi.org/10.1016/j.cub.2016.02.063

Van Der Meij, J., Martinez-Gonzalez, D., Beckers, G. J. L., & Rattenborg, N. C. (2019). Intra-"cortical" activity during avian non-REM and REM sleep: Variant and invariant traits between birds and mammals. *Sleep*, *42*(2), 1–13. https://doi.org/10.1093/sleep/zsy230

van der Meij, J., Rattenborg, N. C., & Beckers, G. J. L. (2020). Divergent neuronal activity patterns in the avian hippocampus and nidopallium. *European Journal of Neuroscience*, *7*, 0–2. https://doi.org/10.1111/ejn.14675

Vyazovskiy, V., Borbély, A. A., & Tobler, I. (2000). Unilateral vibrissae stimulation during waking induces interhemispheric EEG asymmetry during subsequent sleep in the rat. *Journal of Sleep Research*, *9*(4), 367–371. https://doi.org/10.1046/j.1365-2869.2000.00230.x

Vyazovskiy, V. V., Olcese, U., Hanlon, E. C., Nir, Y., Cirelli, C., & Tononi, G. (2011). Local sleep in awake rats. *Nature*, *472*(7344), 443–447. https://doi.org/10.1038/nature10009

Vyazovskiy, V. V., & Tobler, I. (2008). Handedness leads to interhemispheric EEG asymmetry during sleep in the rat. *Journal of Neurophysiology*, *99*(2), 969–975. https://doi.org/10.1152/jn.01154.2007

Wild, J. M. (1987). Thalamic projections to the paleostriatum and neostriatum in the pigeon (Columba livia). *Neuroscience*, *20*(1), 305–327. https://doi.org/10.1016/0306-4522(87)90022-4

Yeganegi, H., & Ondracek, J. M. (2023). Multi-channel recordings reveal age-related differences in the sleep of juvenile and adult zebra finches. *Scientific Reports*, *13*(1), Article 1. https://doi.org/10.1038/s41598-023-35160-1